Reliability Engineering and System Safety 203 (2020) 107079

Contents lists available at ScienceDirect

Reliability Engineering and System Safety

journal homepage: www.elsevier.com/locate/ress

Impact of transmission tower-line interaction to the bulk power system during hurricane

Jiayue Xue[a], Farshad Mohammadi[c], Xin Li[b], Mostafa Sahraei-Ardakani[c], Ge Ou[a,*], Zhaoxia Pu[b]

[a] Department of Civil and Environmental Engineering, University of Utah, Salt Lake City, UT 84112, United States
[b] Department of Atmospheric Sciences, University of Utah, Salt Lake City, UT 84112, United States
[c] Department of Electrical and Computer Engineering, University of Utah, Salt Lake City, UT 84112, United States

ARTICLE INFO

Keywords:
Wind engineering
Wind fragility model
Bulk power network
Transmission system
Hurricanes
Power system reliability
Power system resilience

ABSTRACT

A Hurricane is a severe weather event that has caused massive blackouts in the United States. Previous studies about a hurricane's impact on the power system were mainly conducted through statistical analysis. However, there is limited research that reveals the physical law governing power outage and system-level performance. Therefore, this paper investigates the impact of transmission tower damage and failure on the performance of the power transmission network during a hurricane. To translate meteorological information to the input of the abstract power network, a fragility model of a transmission tower-line considering the coupling effect is developed. The computational efficiency in the fragility analysis is enhanced by wind speed convention and sample size selection. The effectiveness of the fragility model is investigated in a benchmark problem, which evaluates the performance of a synthetic transmission system (Texas 2000-bus power network) during Hurricane Harvey. The promising results indicate that: (1) from both the element and system level, the coupling effect between the transmission tower-line system is not negligible; (2) the computational efficiency of the fragility analysis can be significantly improved by wind speed conversion and sample size selection; (3) considering the tower-line interaction, the estimated damage to the power system matches the recorded damage from Hurricane Harvey.

1. Introduction

A hurricane is one of the major natural hazards that cause dramatic economic, social, and environmental loss. In the 2018 Atlantic hurricane season, Hurricane Michael caused approximately $25 million damage estimated by the National Oceanic and Atmosphere Administration [1]. Widespread power outages affected 1.7 million customers in six states [2]. Meanwhile, power outage also indirectly impacts communication, transportation, medical, and all other lifeline systems. As Abedi et al. [3] summarized in the review, the natural hazard is a significant cause of the power system failure and leave a long-duration impact. Therefore, the reliability analysis of the power system during extreme events draw a lot of researchers' attention: (1) some mathematical approaches such as the sequence operation theory, the fault tree analysis are implemented to evaluate the power system reliability [4,5]; (2) maintenance optimization and hardening strategies are proposed based on the system reliability [6–8]; (3) some comprehensive frameworks are developed to provide the vulnerability indicators [9], rank the critical components [10], and compare different power flow-based models [11]. However, limited research reveals the physical damage in the transmission system infrastructure and also the further impact on the power network performance during a hurricane.

Previous studies of the hurricane impact power system were mainly conducted through statistical analysis to explore key impact factors, including environmental variables or structural variables. Environmental variables include hurricane wind speed, hurricane rainfall, land cover type, tree type, and so on. Liu et al. [12] employed the negative binomial regression model to predict the power outage. They concluded that several important influence factors such as the maximum gust wind speed and affected companies instead of land cover type and soil drainage level. Han et al. [13] also used this regression model to consider both local climatology and geography information. Nateghi et al. [14] examined the environmental variables by random forest method to develop a simplified hurricane power outage forecasting model with fewer variables. Several other statistical analysis models including the spatial generalized linear mixed modeling approach [15] the classification and regression trees approach [16], the quantile regression forests and Bayesian additive regression trees method are also employed to determine the important variables like company indicator covariates, the influence of soil and elevation characteristics and local conditions. Structural variables include the power system

* Corresponding author.
E-mail address: ge.ou@utah.edu (G. Ou).

https://doi.org/10.1016/j.ress.2020.107079
Received 20 November 2019; Received in revised form 2 June 2020; Accepted 17 June 2020
Available online 20 June 2020

components like the transmission line, transmission tower, wood pole, etc. Guikema et al. [17] employed the regression and data mining to estimate the damaged utility poles for the prestorm estimation of a power outage. Liu et al. [18] used a fuzzy inference system combined with the regional weather model to obtain the increment multipliers of the failure rate of transmission lines during the hurricane. However, most research above utilizes a data-based approach to predict the hurricane-induced power outage based on the environmental or structural variable analysis.

Limited research demonstrates the physical laws that govern the hurricane's impact on the power system components and eventual impact on the power outage. A Power system's failure and damage during a hurricane are led by the failures of the physical structural components supporting the power transmission and distribution system [19]. The main structural components of a power system include power plants, substations, transmission towers, transmission lines, and distribution lines [20]. The structural damages in the system during a hurricane can be induced by either heavy wind or flood [21]. Substations are vulnerable due to the flood or storm surge during a hurricane [22]. Transmission tower-line structure system has complex vibration modes; they span a vast geographical region and therefore are fully exposed to the wind field during a hurricane. North American Electric Reliability Corporation (NERC) reports show that Electric Reliability Council of Texas (ERCOT) experienced 106 transmission line outages (138 kV and above) after Hurricane Harvey made landfall [23]. Similarly, Hurricane Sandy caused the outage of over 218 high-voltage (115 kV and above) transmission lines [24]. It can be concluded that the transmission tower-line system is vulnerable to the extensive dynamic wind loading. Among the limited research which predicts the power system performance considering the structural physical damage, Winkler et al. [25] considered power system components' impact on the power outage by HAZUS while they did not involve the critical coupling effect between the transmission tower-line system.

This paper presents a physical based simulation process that estimates the damage and failure of bulk power system, taking the transmission tower-wire structural interaction into account. Previous research about the transmission tower-line system's structural behavior during large wind loadings can be divided into deterministic analysis and probabilistic analysis [26–29]. Deterministic analysis conducted through finite element modeling demonstrates the transmission tower-line structural behavior by static nonlinear analysis [30,31] and wind-induced vibration dynamic analysis [32]. However, the finite element method can only reflect an individual structure's behavior under a certain wind load in a deterministic way. For a specific hurricane event, obtaining the responses of each structure requires a set of simulations for each individual tower. The average response can further take random wind time histories at each tower location into account. However, for a system-level simulation, which hundreds of thousands of towers are included in a target region, such intensive simulation is computationally expensive. It is necessary to reflect the transmission tower-line's structural behavior in a probabilistic way by fragility analysis.

Wind fragility modeling is the most common probabilistic approach utilized [33–35]. The wind fragility model expresses the likelihood of structural damage under different wind intensities and directions [31,36–37]. After the fragility model is developed, the user can rapidly calculate the transmission tower-line system's failure probability with given wind speed and attack angle. The state-of-the-art investigation on the probabilistic performance of transmission tower-line system can be divided into three categories: (1) the fragility model considering only a single tower response; (2) the fragility model only considering a transmission line response; and (3) the fragility model that captures the interaction between transmission tower and line. Fu et al. [38] conducted the single transmission tower's fragility analysis subject to the wind and rain loads. Ma et al. [39] presented a conductor's fragility analysis during a hurricane for the probabilistic simulation of the power system. Fu et al. [40] considered the coupling effect between the transmission tower and line by a simplified model. Cai et al. [41] developed the fragility modeling framework for a transmission tower-line system by considering the line load. However, the fragility analysis considering the coupling effect of the transmission tower-line system is limited.

Challenges exist in developing a fragility model for a transmission tower-line system. These include: (1) due to unevenly distributed stiffness of a transmission tower and the largely geometrical nonlinearity of the long transmission line, the transmission tower-line system's dynamic response is complex; the model reduction and simplification are challenging to achieve with high fidelity. (2) The dynamic analysis of the transmission tower-line system during intensive wind is usually realized by implicit Newmark-β method in ANSYS [32]; when solving the nonlinear problem, this integration method is difficult to converge. (3) As fragility analysis shows the structure's failure probability subject to a certain wind load, a set of simulations is needed for the probabilistic analysis. To obtain the transmission tower-line system's high order response, each simulation case takes several hours to run. The fragility analysis is computationally expensive [42–44].

To address the aforementioned challenges, this paper uses an explicit integration method to analyze the transmission tower-line system's dynamic response under intensive wind loads. Meanwhile, the computational efficiency of the fragility analysis is improved by wind speed conversion and optimal sample size selection. The transmission tower-line system fragility model is compared to the fragility model of only the transmission tower. We further investigate the impact of the transmission tower-line interaction on the system level performance of a transmission power network. A benchmark problem that simulates the performance of a synthetic power network during Hurricane Harvey is used to conduct the system-level analysis.

2. Transmission tower-line system modeling during intensive wind

The objective of the structural model is to map the damage condition of a transmission tower to the wind field information (wind speed, wind direction), which enables the performance analysis of the power system. To develop a wind fragility model which represents the failure probability of the transmission tower due to different loading conditions, the first task is to analyze the dynamic response, failure modes, and limit states of a transmission tower during intense winds considering the tower-line interaction (Fig. 1).

2.1. Model information of the prototype transmission tower-line system

The transmission tower investigated in this paper is a suspension tower designed for Texas with a height of 31.5 m, steel-made members (ASTM A-36), and L-shaped cross-sections. The transmission tower is initially described by Tort et al. [45] and redesigned based on ASCE

Fig. 1. Reported 345 kV line structure down during hurricane Harvey [23].

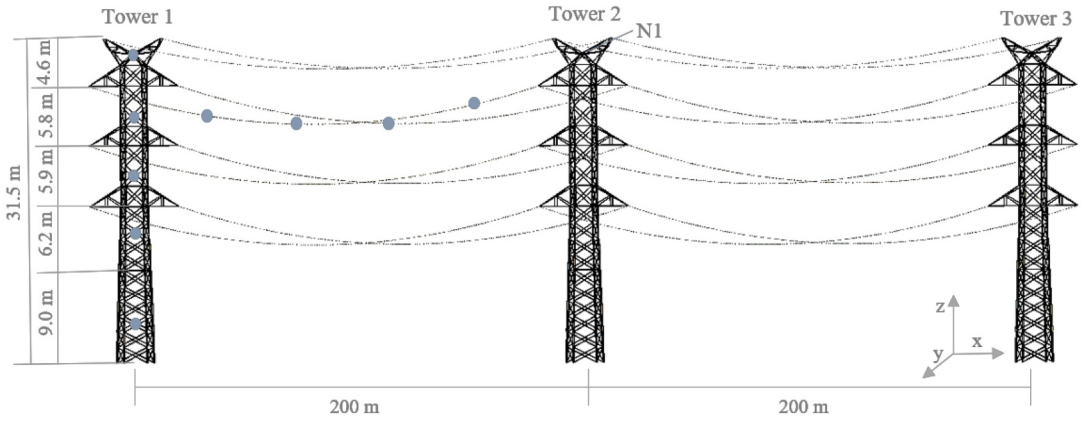

Fig. 2. Finite element model of transmission tower-line system.

Manual 74 Guidelines for Electrical Transmission Line Structural Loading [46] using the industry-standard software PLS-TOWER. Based on research by Zhang et al. [32], a three-tower two-line model is a good representation of the transmission tower-line system. Hence, this paper develops a prototype three-tower two-line model to capture the interaction between the transmission tower and line. In the prototype simulation, the span between the two towers is determined at 200 m. The maximum sag of the ground line and the conductor is 2.9 m and 3.7 m, respectively. Fig. 2 displays the finite element model of a transmission tower-line system. Design details of the transmission tower-line system are provided on the WeatherG website [47].

We used ANSYS LS-DYNA to develop the finite element model of this transmission tower-line system. ANSYS LS-DYNA is a commonly used explicit dynamic response analysis program to model the mechanical phenomena with high nonlinearity [48]. Compared with the implicit integration, based on commercial software using the transient analysis and implicit integration, the explicit integration method does not need to form the global stiffness matrix, which facilitates convergence. It is a proper way to simulate a complex and nonlinear structural dynamics system [49]. The tower members are modeled as beam 161, and the line members are considered as truss elements.

Determining the initial configuration of the transmission line is significant for developing a finite element model for it. The spatial shape equation of the transmission line can be determined by Eq. (1) [32,50], as the span sag ratio of the transmission line is less than $\frac{1}{8}$.

$$z = \frac{q}{2H}x(l-x) + \frac{c}{l}x,\ \ H = \frac{ql^2}{8f} \tag{1}$$

where z and x are the spatial coordinates, q is the line weight, H is the initial horizontal tension, l is the span, c is the height difference, and f is the sag of the transmission line, respectively.

2.2. Dynamic wind simulation

The dynamic wind, composed of the mean and fluctuating wind, is simulated and added on the transmission tower-line system as input loading. The fluctuating wind is simulated based on the mean wind. In ASCE 7-93, mean wind profile changes over height by a power law [38,51].

$$\frac{\bar{V}}{\bar{V}_{10}} = \left(\frac{z}{z_{10}}\right)^{\alpha} \tag{2}$$

where $\bar{V}$ is the mean wind speed along with the height; $\bar{V}_{10}$ is the mean wind speed at 10 m height; z is the height of the mean wind speed and z_{10} is the reference height, 10 m; α is the surface roughness coefficient for the open terrain.

As the mean wind is obtained by the power law, the fluctuating wind can be expressed as a Gaussian stationary random process. For an n-dimensional zero-mean stationary Gaussian random process $v_j(t)(j = 1, 2, \ldots, nt)$, the spectral density matrix is shown in (3).

$$S(\omega) = \begin{bmatrix} S_{11}(\omega)S_{12}(\omega)\cdots S_{1n}(\omega) \\ S_{21}(\omega)S_{22}(\omega)\cdots S_{2n}(\omega) \\ \cdots \\ S_{nt1}(\omega)S_{nt2}(\omega)\cdots S_{ntnt}(\omega) \end{bmatrix} \tag{3}$$

Davenport spectrum is used to obtain the power spectrum of fluctuating wind [38,40,52]. It is a spectrum implemented to generate the dynamic wind on the transmission tower or line [38,40] when the local measured spectrum is not available. The auto power spectrum of fluctuating wind is obtained by (4).

$$S_v(f) = 4\kappa\bar{V}_{10}^2\frac{x^2}{f(1+x^2)^{4/3}}\ x = \frac{1200f}{\bar{V}_{10}} \tag{4}$$

where $S_v(f)$ is the auto power spectrum of the fluctuating wind at frequency f. κ is the surface drag coefficient.

The spatial correlation of the fluctuating wind is obtained by its cross-spectral density spectrum $S_{ij}(r,f)$ based on each panel's auto power spectrum from Eq. (4).

$$S_{ij}(r,f) = \sqrt{S_{ii}(z_i,f)S_{jj}(z_j,f)}\,Coh(r,f),\ \ i \neq j \tag{5}$$

$$Coh(r,f) = exp\left(\frac{-2f\sqrt{C_y^2(y_i-y_j)^2 + C_z^2(z_i-z_j)^2}}{\bar{V}(z_i)+\bar{V}(z_j)}\right) \tag{6}$$

where $C_y = 8$ and $C_Z = 7$. y_i, y_j, z_i and z_j are the spatial coordinate. It is decomposed by Cholesky decomposition.

$$S(\omega) = H(\omega)H^*(\omega)^T \tag{7}$$

$$H(\omega) = \begin{bmatrix} H_{11}(\omega)\ 0\ \cdots\ 0 \\ H_{21}(\omega)H_{22}(\omega)\ \cdots\ 0 \\ \cdots\cdots\cdots \\ H_{nt1}(\omega)H_{nt2}(\omega)\cdots H_{ntnt}(\omega) \end{bmatrix} \tag{8}$$

Fluctuating wind $v_j(y_j, z_j, t)$ can be obtained after this.

$$v_j(y_j, z_j, t) = \sqrt{2(\Delta\omega)}\sum_{m=1}^{j}\sum_{l=1}^{N}|H_{jm}(\omega_{ml})|\cos(\omega_{ml}t - \theta_{jm}(\omega_{ml}) + \varphi_{ml})\ j = 1, 2, \ldots, nt \tag{9}$$

$$\omega_l = (l-1)\Delta\omega + \frac{m}{N}\Delta\omega,\ \ l = 1, 2, \ldots, N \tag{10}$$

where $H(\omega)$ is the decomposed matrix by Cholesky decomposition; $\Delta\omega$ is the frequency increment; N is a large positive integer.

Since there are 5403 nodes in the transmission tower-line system, it is necessary to select several representative nodes to generate the wind speeds and add the wind load. As demonstrated in Fig. 2, we divided each transmission tower and each transmission line into several parts,

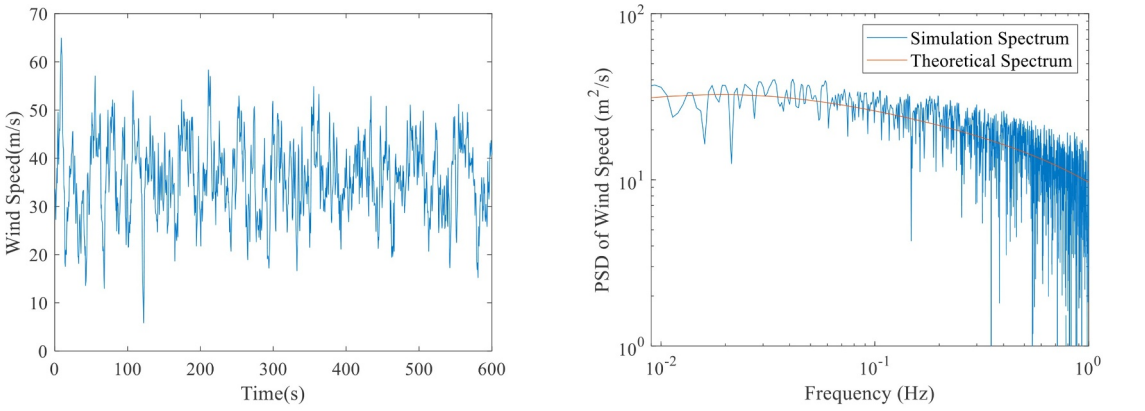

(a) Wind Speed at Top of First Tower

(b) Comparison between Simulate Spectrum and Davenport Spectrum

Fig. 3. Wind speed simulation and spectrum comparison.

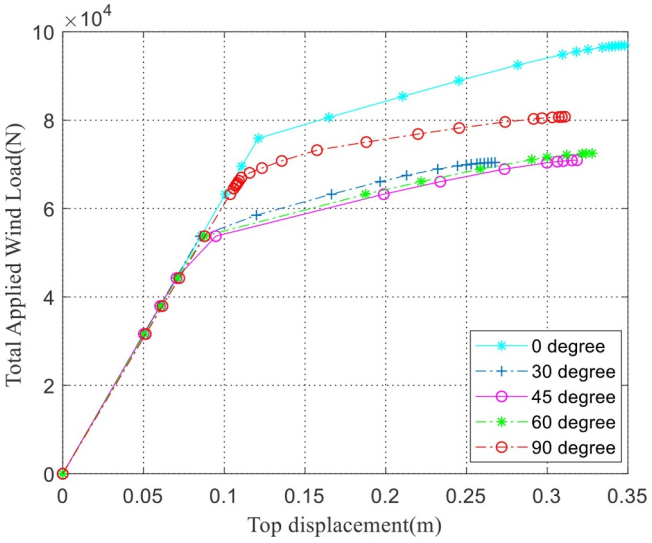

Fig. 4. Capacity curve of transmission tower.

respectively. The generated point wind loads will be added on the selected nodes of the transmission tower-line system. Fig. 3(a) demonstrates the simulated wind speed at the top of the first tower when the mean wind speed is 30 m/s at 10 m height. Fig. 3(b) is the comparison between the simulated spectrum and the Davenport spectrum.

Wind pressure in a wind field is calculated as Eq. (11) [53].

$$q_z = 0.5\rho V(t)^2 \tag{11}$$

Wind load is related to the wind pressure, air density, and drag coefficient in Eq. (12).

$$F = q_z C_f A_m \tag{12}$$

where ρ is the air density, chosen as 1.195 kg/m^3. $V(t)$ is wind time history, obtained from Eqs. (2) to (10). C_f is the drag coefficient, and A is the projected area. Drag coefficients of the transmission tower are calculated based on the solidity of transmission tower from Tables 2 to 4 in ASCE Manual 74 [46]. The drag coefficient of the transmission line is recommended as 1.0.

2.3. Transmission tower-line failure analysis and limit state evaluation

In order to conduct the fragility analysis of the transmission tower-line system, the failure criterion of the tower-line system should be identified first. This paper employs the nonlinear static pushover (NSP) method [54] to obtain the transmission tower's capacity curve, which is then used as the reference to generate the fragility curve. Static wind load is calculated in Eq. (13) and (14) based on ASCE Manual [46].

$$F_t = \gamma_w Q K_z K_{zt} V^2 G_t \cos\Psi C_{ft} A_{mt} \tag{13}$$

$$F_l = \gamma_w Q K_z K_{zt} V^2 G_t \sin\Psi C_{fl} A_{ml} \tag{14}$$

where γ_w equals 1.0 in this paper, which is the load factor related to wind return period; Q is a numerical constant, 0.00256; K_{zt} is the topographic effect coefficient, which equals 1.0 in a plain area; V is the wind speed and G_t is the gust response factor; Ψ is the yaw angle in a horizontal plane. C_{ft} and C_{fl} are drag coefficients related to the face of structure, which is parallel and perpendicular to the line. A_{mt} and A_{ml} are all member areas in the face of structure, which are parallel and perpendicular to the line, respectively.

To consider the power system's performance during a hurricane, five wind attack angles Ψ: 0°, 30°, 45°, 60° and 90° are chosen. Degree of 0° is the wind direction along the axis of the transmission line (x-axis) and an attack angle of 90° is for the case, where the wind direction acts perpendicular to the line direction (y-axis) as Fig. 2 displays. By monotonically increasing wind load, the force and deformation curve, i.e., the capacity curve is obtained, as shown in Fig. 4.

The top displacement of the transmission tower is always considered as a convenient index to reflect the tower's dynamic response [55]. In addition, the transmission line rarely gets pulled apart during hurricanes [56]. Hurricane's impact on the transmission tower-line system is the tension on the tower caused by the lines. Therefore, this paper chooses the top displacement of the middle tower, as N1 in Fig. 2, to evaluate the transmission tower-line system's limit state. As Fig. 4 shows, the failure of the transmission tower occurs when the capacity curve reaches its limit [54]. Hence, at these five wind attack angles, the transmission tower reaches its limit state when the top displacement is around 0.27 m to 0.35 m, which is equivalent to a drift ratio between 0.86% to 1.1%. This paper chooses the top drift 1% of the transmission tower as the limit state to evaluate the failure of the tower.

3. Fragility analysis of transmission tower-line system considering tower-line interaction

Since the transmission tower-line system's dynamic response is complex and computationally burdensome, the computational efficiency improvement for the fragility analysis of the transmission tower-line system is critical.

3.1. Computational efficiency improvement for fragility analysis

As stated above, the fragility curve displays the likelihood of damage of the structure as a function of different wind speeds. Thus, this paper investigates the transmission tower-line system's failure probability from the mean wind speed at 10 m height changing from 15 m/s to 70 m/s with 5 m/s intervals. There are 12 groups of mean wind speed. At each mean wind speed group, a set of mean wind speed in $a \pm 2$ m/s range by Monte-Carlo simulation is considered for the stochastic process.

To determine the computational time in running each dynamic response simulation, a test was conducted on a computer with an Intel (R) Core (TM) i7-8700 CPU and 64.0 GB RAM. The results show that more than 9 h are needed to calculate the dynamic response of the transmission tower-line system under a 60 s wind loading input. Meanwhile, using Monte-Carlo simulation, to take the stochastic effect of wind loading into account, results in hundreds of simulations at each wind speed. Considering different attack angles will only add to the computational burden of developing the fragility model. Consequently, it is critical to find a computationally efficient way to generate the fragility curve. This paper focuses on two aspects: wind speed conversion and determining the optimal sampling size for the Monte-Carlo simulation.

According to ASCE Manual 74 [46], the wind speed values depend on the wind speed record on the averaging time. Higher wind speed corresponds to a shorter averaging time, and lower wind speed corresponds to a longer time. Therefore, it is reasonable to employ the mean conversion figure, reported by Durst [57] to transfer the mean wind speed from 600 s to a shorter time. Here in Fig. 5 the horizontal axis is the averaging time of the wind speed, and the vertical axis is the ratio V_t/V_h, as the wind speed is averaged in t seconds to hourly mean wind speed. Therefore, a ratio of 3-second wind speed V_{3s} to 10-minute wind speed V_{10min} at 10 m, $V_{3s}/V_{10min}$is roughly 1.43 (where $V_{3s}/V_h = 1.526$, $V_{10min}/V_h = 1.067$ from Fig. 5).

To obtain a proper short time period with higher accuracy, we generated 100 samples for the mean wind speed ranging from 25 m/s to 75 m/s with different time windows: 3 s, 5 s, 10 s, 15 s, 20 s, and 600 s. We further investigated the mean maximum top displacement of the tower by averaging the maximum displacement of the tower during each wind loading sample with different time windows. Table 1 illustrates the mean top displacement results of this comparison. As the Davenport spectrum used to simulate the fluctuating wind is obtained in 8–10 min time period [52], this paper takes 600 s as a reference to compare the result. It clearly shows that when transferring the wind speed in 600–5 s, the absolute errors of the tower's top displacement are all below 10%. The mean absolute error (MAE) is only 3.81%. Thus, it is reasonable to employ this wind speed conversion from 600 s to 5 s to simulate the transmission tower-line system's dynamic response in a short period with high accuracy.

Another way to reduce the calculation time is to choose a proper sample size to capture the stochastic wind loading through Monte-Carlo simulation. This paper compares the results from 20, 50, 80, 100, and 200 samples for the transmission tower's fragility curve. Fig. 6 displays the results, which show that the fragility curves of the five sample sizes are similar. According to the sample size 20, 50, 80, 100, 200 of the Monte-Carlo simulation, the failure probability resolution of each sample size is 0.05 (1/20 samples), 0.02(1/50 samples), 0.0125(1/80 samples), 0.01(1/100 samples), and 0.005(1/200 samples). The discrepancy of different sample size's failure probability at 40 m/s and 50 m/s is mainly because of this resolution difference: 0.05, 0.02, 0.0125, 0.01, and 0.005 from the sample size. Besides, the difference is also acceptable because the fragility curve for the same tower in the same sample size will get slightly different fragility curve when running Monte-Carlo simulation several times.

3.2. Fragility curve of transmission tower-line system

Based on the effective fragility analysis stated above, the fragility curve of the transmission tower-line system can be calculated. In structural wind fragility analysis, the damage and failure probability $F_R(V)$ under a given wind speed V is determined by Eq. (15):

$$F_R(V) = P[l > LS|\bar{V}_{10} = V], \tag{15}$$

where LS is the limit state discussed in Section 2.3; l is the simulated response compared with the limit state; in the development of the transmission-line system fragility curve, l is the top displacement of the middle tower in this analysis. $\bar{V}_{10}$ is the mean wind speed at 10 m ranging from 15 m/s to 70 m/s with 5 m/s increase. At each wind speed, the sample size is 20, as discussed in Section 3.1. If the top displacement of the middle tower is larger than the limit state 1% drift at each case, it is considered failed. The failure probability is calculated as the number of failed transmission towers over total 20 cases at each wind speed. The fragility curve is formed based on all the failure probabilities of each wind speed. The fragility curve of the transmission tower-line system is presented in Fig. 7(a). Developing the fragility curve of a stand-alone transmission tower (not considering the tower-wire interaction) is a standard process [58]. Fig. 7(b) is a comparison between the stand-alone transmission tower's fragility curve with the transmission tower-line system's fragility curve. It demonstrates that the interaction between the transmission tower and line impacts the performance of the transmission tower significantly. Stand-alone

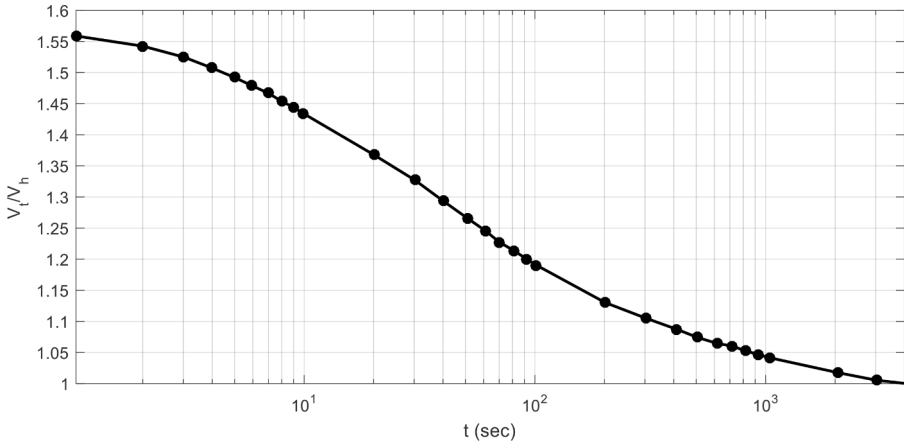

Fig. 5. Regeneration of the wind speed conversion [57].

Table 1
Error analysis of tower's top displacement (m) in different time periods.

Time	600s	3s		5s		10s		15s		20s	
Coefficient[1]	1.08	1.529	Absolute Error	1.5	Absolute Error	1.44	Absolute Error	1.4	Absolute Error	1.371	Absolute Error
Conversion Coefficient[2]	1	1.42	(%)	1.39	(%)	1.33	(%)	1.3	(%)	1.27	(%)
25 m/s_100	0.1383	0.1304	5.71	0.1333	3.62	0.1477	6.80	0.1507	8.97	0.1552	12.22
30 m/s_100	0.198	0.1848	6.67	0.1953	1.36	0.2132	7.68	0.224	13.13	0.2711	36.92
35 m/s_100	0.2766	0.2496	9.76	0.2658	3.90	0.2937	6.18	0.3088	11.64	0.3063	10.74
40 m/s_100	0.366	0.3482	4.86	0.353	3.55	0.3963	8.28	0.4204	14.86	0.4127	12.76
45 m/s_100	0.467	0.4353	6.79	0.4603	1.43	0.5144	10.15	0.5353	14.63	0.5191	11.16
50 m/s_100	0.5631	0.5121	9.06	0.5525	1.88	0.6353	12.82	0.6467	14.85	0.6909	22.70
55 m/s_100	0.7124	0.6489	8.91	0.6949	2.46	0.7498	5.25	0.8025	12.65	0.8263	15.99
60 m/s_100	0.8514	0.7708	9.47	0.7825	8.09	0.9526	11.89	0.8968	5.33	0.9349	9.81
65 m/s_100	1.0034	0.9069	9.62	0.9537	4.95	1.0716	6.80	1.1034	9.97	1.1471	14.32
70 m/s_100	1.1669	1.0441	10.52	1.0628	8.92	1.2843	10.06	1.3293	13.92	1.3386	14.71
75 m/s_100	1.3474	1.1889	11.76	1.3243	1.71	1.4146	4.99	1.5092	12.01	1.5099	12.06
MAE[3]	–	–	8.47	–	3.81	–	8.26	–	12.00	–	15.76

Note: Coefficient[1] is the ratio, V_l/V_h (Durst, 19,610); Conversion coefficient[2] is to consider 600 s as the reference time period, the conversion factor converts the wind speed in other time period to 600 s; MAE is the mean absolute error.

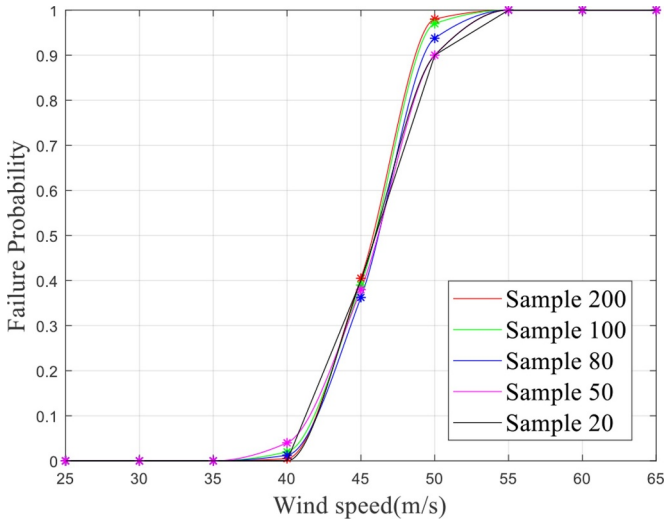

Fig. 6. Fragility curve of different sample size (transmission tower).

transmission tower starts to fail much later than the transmission tower-line system, which can lead to overly optimistic results for the power system performance assessment.

4. Power system performance considering tower-line interaction during hurricanes

In order to investigate the impact of transmission infrastructure performance on transmission power network during the hurricanes, the structural model should be integrated into a system-level simulation platform. We utilized a wind-impacted power system performance simulator in this research. The simulator includes four modules: (1) a hurricane wind field information module, which produces the realistic wind data, including the wind speed and direction, in a grid format in the region of the study; (2) a physical power system module which maps a power network to the physical region of the study; the physical power system infrastructure includes generators, substations, and transmission towers and lines designed for the study region; (3) a transmission system structural performance analysis module which integrates the physical transmission system infrastructure, the structural models, and the wind field information to estimate the damage and failure likelihood of each individual structure inside the study region; for individual transmission tower-line structural systems (three-tower two-line system), the component failure probability will be converted to the failure and damage of a transmission line (which is composed of hundreds of towers); (4) power network simulation module which utilizes stochastic analysis to simulate the probabilistic power outage and economic loss due to the physical damage to the infrastructure, after obtaining the damage and failure probability of the physical

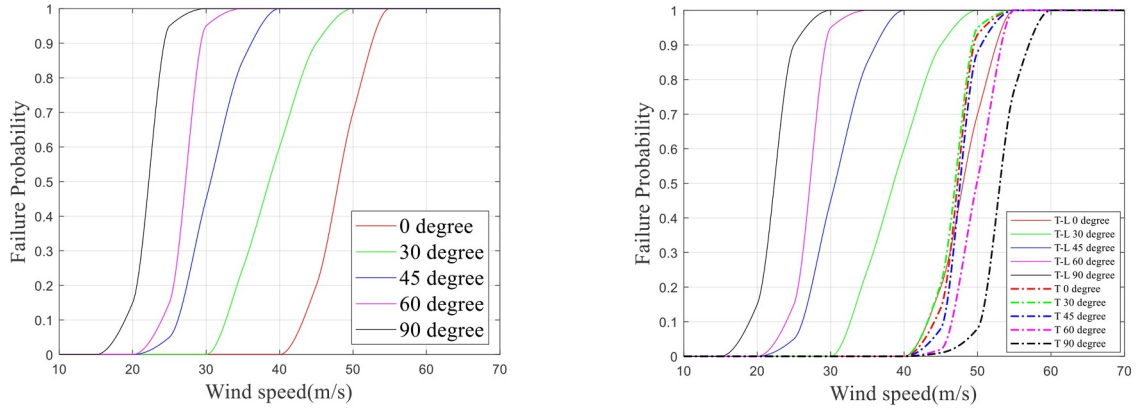

(a) Fragility Curve of Tower-line System at Different Wind Attack Angle

(b) Fragility Curve Comparison between Tower-Line System and Single Tower

Fig. 7. Fragility curve of transmission tower-line system and single tower.

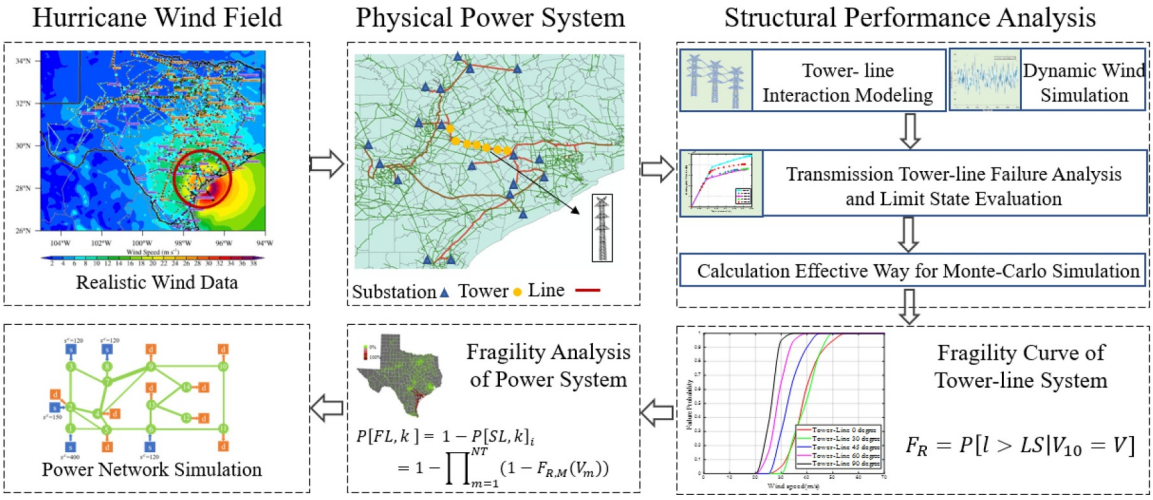

Fig. 8. Wind-impacted bulk power system performance simulator.

components in the transmission power system. The workflow of the wind-impacted power system performance simulator is demonstrated in Fig. 8.

In the benchmark problem, the simulator evaluates the performance of a synthetic power network during Hurricane Harvey. In the wind filed information module, the wind field is calculated based on the observed wind speed and direction for Hurricane Harvey. We mapped the designed transmission-line structural system is mapped to a synthetic Texas 2000-bus network model [59] to the footprint of Texas.

The damage and failure probabilities of the transmission-line system are predicted, and the element failure of transmission-line is estimated according to both (1) the structural model only considering individual towers and (2) structural models considering the tower-line interaction. To investigate the system-level performance, the power network simulation module predicts the power outage and economic loss for both cases. To be noted, multiple designs and multiple spans are not yet fully considered in the study. The main reason is due to the missing design blueprints of transmission tower in different voltage, and the span variation and performance of the transmission tower would be affected to the detailed topography. However, as the objective of this study is to evaluate the impact of the transmission tower-line interaction, the simplified assumption of using a universal tower and span design throughout the entire system is considered to be valid. The detailed results in each module are presented in the following subsections.

4.1. Hurricane wind field information and the studied region

To obtain a high-resolution hurricane wind field information, a mesoscale community Weather Research and Forecasting (WRF) Model (https://www.mmm.ucar.edu/weather-research-and-forecasting-model), which is a numerical weather prediction system designed for both atmospheric research and operational forecasting applications, is employed to simulate the hurricane during its landfall period. The National Centers for Environmental Prediction (NCEP) Global Forecast System (GFS) final analysis (FNL) are used to generate meteorological input data for the WRF model. These NCEP 0.25-degree by 0.25-degree grid (about 27.8 km × 27.8 km) FNL data is produced from the Global Data Assimilation System (GDAS), which continuously collects observational data from the Global Telecommunications System (GTS) and other sources for analyses. To produce flexible meteorological data for this study, the FNL data, as well as Moderate Resolution Imaging Spectroradiometer (MODIS) collected land cover data are input into the WRF model during the simulation. The WRF model generates a meteorological field data hourly with a horizontal resolution of 1 km. Fig. 9 displays a sample of the wind field of Hurricane Harvey.

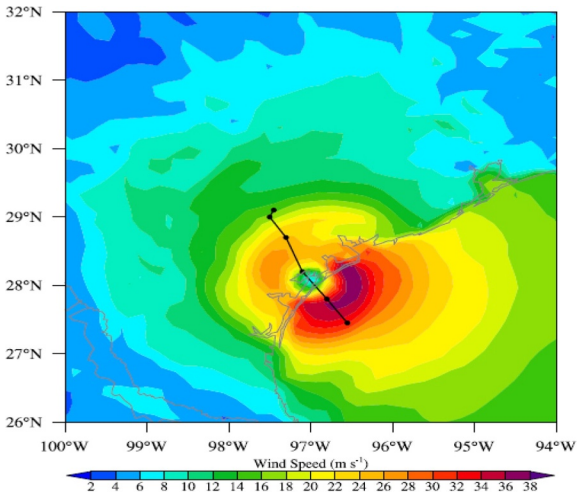

Fig. 9. Hurricane wind field in Texas.

Hurricane Harvey mainly attacked the coastal area, and the wind speed inland was relatively small, compared with the wind speeds when it had been over the ocean. Hurricane wind field is simulated from 26° N to 36° N and 94° W to 100° W. This wind field information includes the mean wind speed at 10 m height and the movement from August 25th 4:00 p.m. to August 26th 4: 00 p.m. Fig. 9 demonstrates the hurricane wind field data in Texas at 1 a.m., August 26th.

4.2. Mapped power system

According to the hurricane's landfall position and influenced area, the local power system should be mapped to the corresponding geographical location. Power networks are usually described by three elements: (1) the network bus, which describes nodes in the system; (2) the generator, which contains information of the generator's nodal location, limits and cost data; and (3) the transmission data, which describes the links connecting two nodes of the network. To simulate a more realistic power outage case, this paper employs the ACTIVSg 2000: a synthetic 2000-bus Texas power system test case, to conduct the simulations [59], as demonstrated in Fig. 10. This Texas 2000-bus system is built on the footprint of the Electric Reliability Council of Texas (ERCOT) to provide similar generation and load profiles while it has no relation to the actual grid in Texas. In this power system, every point represents a substation, and each transmission line links the substations. The locations of the substations are provided by this test

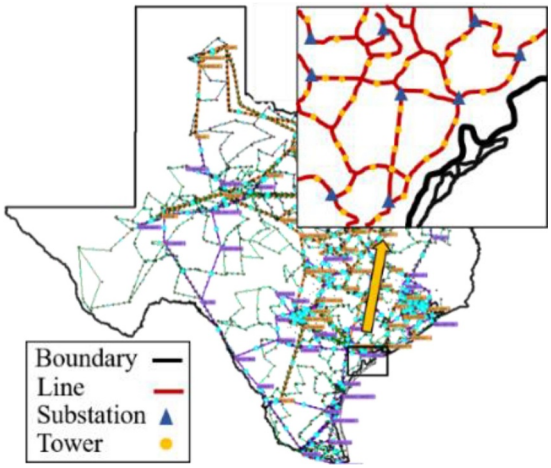

Fig. 10. Mapping geographical information and structural components to Texas 2000 bus system.

system. All the transmission tower-line have the same tower type and span as shown in Fig. 2.

4.3. Transmission system structural performance analysis

As the simulated wind field and the power system in the hurricane influenced area is determined, the mean wind speed and wind attack angle on each transmission tower is obtained (Fig. 11). The arrows represent the wind direction. Assuming that the longitude is the horizontal direction, the wind direction and the transmission line's direction to the horizontal direction are β and α, respectively. The wind attack angle to the transmission tower-line system is θ.

By giving the wind attack angle and the wind speed from the hurricane wind field, the damage probability for each transmission tower can be estimated based on the structural fragility model of the transmission tower-line structural system, as developed in Section 3.2. A transmission line is composed with hundreds of towers, which is a serial system. The transmission line survives a wind load only if all of its towers withstand the wind. Each transmission line's current failure is calculated based on the m^{th} individual transmission tower's failure probability $P_m = F_{R,m}(V_m)$ from previous fragility model. The Kth transmission line's ith current independent failure probability is denoted by $P[FL, k]_i$ and its survival probability is $P[SL, k]_i$. FL is each transmission line's failure probability, and k represents the transmission line's index. Thus, the failure probability is calculated as:

$$P[FL, k]_i = 1 - P[SL, k]_i = 1 - \prod_{m=1}^{NT} (1 - F_{R,m}(V_m)) \tag{16}$$

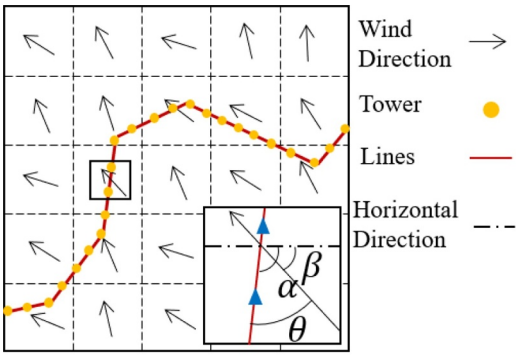

$$\theta = \alpha - \beta$$

Fig. 11. Wind attack angle on transmission tower-line system.

Meanwhile, the passage of the hurricane is a stochastic process. Each transmission line's failure probability at the current time step is dependent on its failure probability in the previous time step. Here, t_i represents the current time step and t_{i-1} is the previous time step. Therefore, each transmission line's dependent failure probability is demonstrated in Eq. (17):

$$P[FL, k, t_i] = P[FL, k, t_{i-1}] + P[SL, k, t_{i-1}] \cdot P[FL, k]_i \tag{17}$$

There are 3206 transmission lines and transformers in Texas 2000 bus system. The failure probability of each transmission line at different time intervals is shown in Fig. 12. After Hurricane Harvey makes landfall, with the movement of the hurricane, transmission lines are damaged gradually. The green line means the transmission line survives the wind. With the color turning red, the failure probability of the transmission line increases. Table 2 summarizes the number of failed transmission lines during different time periods. There are 51 transmission lines with failure probability larger than 90% when the hurricane passes the coastal area of Texas, the failure ratio (failed transmission line over the total transmission lines) is 1.59%.

If the system-level modeling only considers the stand-alone transmission tower performance without the tower-line interaction, and uses the fragility model of the stand-alone transmission tower, only 2 transmission lines are damaged. The calculated probability of failure of these two lines is about 0.6%, as demonstrated in Fig. 13. Such results severely underestimate the damage of the power system. Therefore, it is essential to consider the coupling effect of the transmission tower-line system from the system-level analysis.

North American Electric Reliability Corporation (NERC) reports show that Electric Reliability Council of Texas (ERCOT) experienced 106 transmission line outages (138 kV and above) after Hurricane Harvey made landfall [14]. Texas 2000 bus system is a synthetic system, developed from public data, where the grid location and the number of lines is different from the real system. The realistic Texas system has 7800 transmission lines, and the damage ratio of the transmission line is 1.35%. The percentage of damaged transmission lines, in our simulations, matches the realistic condition.

4.4. Power network performance simulation

The power outage simulator estimates the power outage (unserved load) based on the predicted damage to the power system components. Temporal and geographical distribution of power outage depends on the generation dispatch as well as the level of damage to the network. Generation dispatch simply identifies the commitment status (on or off) as well as the production level of those generators that are on, throughout the duration of operation, which in this paper is a full day. Different dispatch combinations will use the transmission network differently, and thus, will result in different outage distribution even with the same level of damage. In power system operation, day-ahead generation dispatch is calculated using a unit commitment model, which minimizes the cost of operation by finding the cheapest dispatch, while considering the physical constraints of the system. One set of such constraints include the modeling of power flows on transmission lines and the capacity constraints of the transmission system.

To properly estimate the power outages induced by the hurricane, we first solve a unit commitment model, without considering the hurricane impacts. This is referred to as the business as usual scenario. Using the commitment results (hourly generation status and production for each generating unit), the hurricane is simulated in the next stage. Please note that the operators cannot change the status of the generators in real-time, as starting up new generation can take hours depending on the type of the generator. However, the operators can adjust the production levels in response to real-time conditions, such as the damages induced by the hurricane, as long as the changes are within the ramping capabilities of the generators. As the hurricane damages more transmission lines, the operator will change the generation

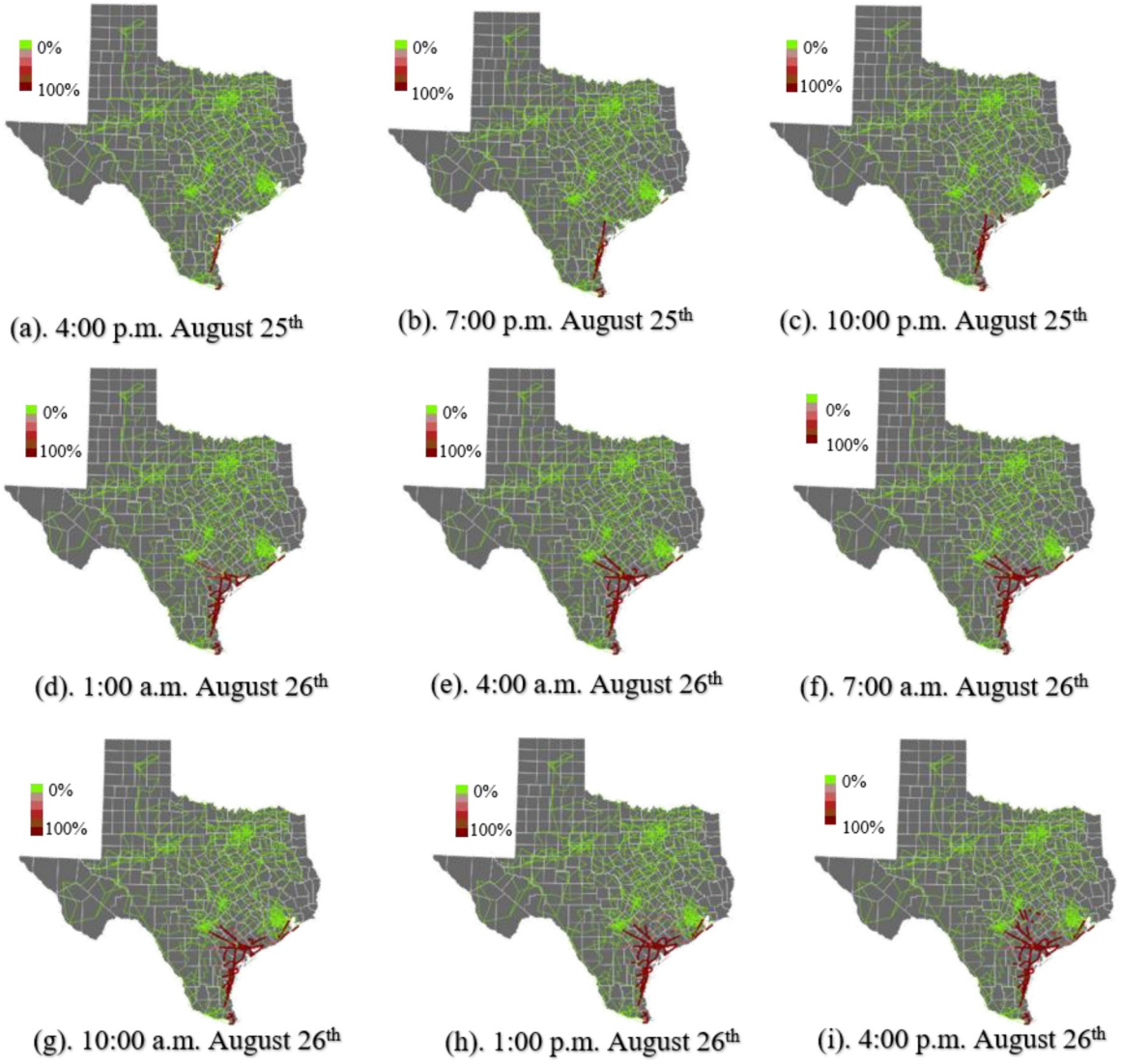

Fig. 12. Transmission line's failure in Texas 2000 bus system considering tower-line interaction.

Table 2
Number of failure transmission lines in different time period.

Time	Number of Failed Lines ($P \geq 0.5$)	Number of Failed Lines ($P \geq 0.75$)	Number of Failed Lines ($P \geq 0.9$)	Total Failed Lines ($P > 0$)
Aug 25th 4:00 p.m.	7	5	5	18
Aug 25th 7:00 p.m.	18	17	10	46
Aug 25th 10:00 p.m.	34	30	25	85
Aug 26th 1:00 a.m.	63	56	51	104
Aug 26th 4:00 a.m.	78	73	68	124
Aug 26th 7:00 am	89	80	72	139
Aug 26th 10:00 a.m.	93	82	73	145
Aug 26th 1:00 p.m.	99	88	78	161
Aug 26th 4:00 p.m.	109	99	87	174

dispatch, without changing the commitment, to minimize the power outage and serve as much load as possible. With few damaged lines, there is a chance to keep the balance and serve the majority of the electricity demand. However, during major hurricanes, the number of damaged lines is too large, and some level of a power outage is unavoidable.

The temporal failure probability for each transmission line is given in the results of the previous section. Considering that there are many transmission lines in this test case (3206 lines), and time resolution of power simulator (3 h), the number of possible network topologies that can emerge due to the hurricane damage is an extremely large number. Here, each unique possibility is referred to as a “future”. It is not possible to simulate each feature to evaluate the unserved load in all of the futures, because of the large number of possible futures. As an alternative solution, Monte Carlo simulation is used to simulate as many futures as possible. In this process, thousands of those futures are selected randomly, and the expected value of power outage is calculated for each future. We stop the Monte Carlo simulations once the average value of the power outage stays stable for at least more than half of the simulations.

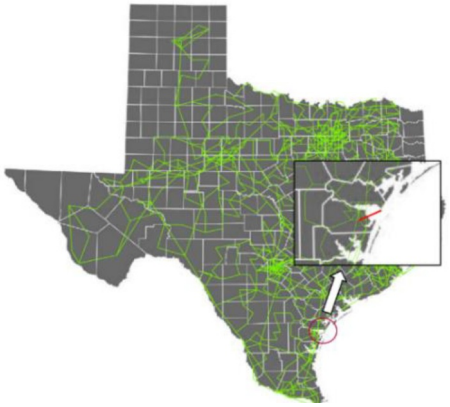

Fig. 13. Transmission line's failure in Texas 2000 bus system only considering single tower.

Table 3
Results for the business as usual case.

Operation Cost	Unserved Load	Over-Generation
20.2 Million $	0.0 MWh	0.0 MWh

Table 4
Expected values when the hurricane affects the network.

	Operation Cost	Unserved Load	Over-generation
Average Value	1701 Million $	42,214 MWh	14,376 MWh
Maximum	1847 Million $	46,518 MWh	15,583 MWh
Minimum	1562 Million $	38,045 MWh	13,448 MWh

In Monte Carlo simulations, for each unique network topology (caused by the hurricane), the commitment status of generating units is fixed. The simulator, then minimizes the unserved load, by adjusting the dispatch within the ramping limits. The unit commitment solution, obtained for business, as usual, would result in no power outage, if the network is not damaged. The power system performance for the business as usual case is shown in Table 3, considering no damage.

During the hurricane, the network will be partially damaged, and some transmission lines will go out of service. The total number of lines with a nonzero damage probability is 174 according to Table 2. Moreover, the hurricane can create islands in the network, which would divide the network into regions that are not connected to each other, with the main network and a number of small islands. Under such conditions, avoiding unserved load and/or over-generation will not be possible. The results of over 1000 Monte Carlo simulations, are presented in Table 4, evaluating the power system performance using the damage probabilities calculated in the previous section.

Table 4 shows that the hurricane leads to high levels of unserved load and over-generation. The total level of load shedding and over-generation is more than 4.4% of the total load in the network. Moreover, the operation cost in this case increased substantially, due to the high penalty for unserved load, which here is considered to be $30,000 per MWh.

5. Conclusions and future work

Hurricane-induced power network damage is a severe issue. Although there is some research about the bulk power system performance analysis during a hurricane, there is limited research that considers the physical laws governing the power outage and system-level performance. In this paper, we presented the physical-based process in estimating the bulk power system performance during a severe wind. Through this framework, we investigated one of the most vulnerable structural components in the bulk power system during a hurricane, which is the transmission tower-line system. We considered the transmission tower-line interaction and studied its impact on the power system performance during a hurricane. A benchmark problem evaluated a synthetic power network in Texas during Hurricane Harvey. The results indicate that the damage of the power system is massively underestimated if only isolated and stand-alone transmission tower or line structural models are considered. It is necessary to take the interaction between towers and line into consideration. In summary, the contributions of this work include:

(1) The fragility model of the transmission tower-line system is developed to probabilistically describe the power system component's failure and damage state.
(2) The computational efficiency of the fragility analysis of the transmission tower-line system is improved. By the error analysis of the wind speed conversion and the sensitivity analysis of the sample size choice, the effective method can largely improve the computational efficiency.
(3) Realistic hurricane wind field information from Hurricane Harvey is utilized in the benchmark problem. Combining with the realistic wind field information, the transmission tower-line structural system fragility model predicted the damage state of the physical elements in the transmission system.
(4) At the system level, the results from the benchmark problem are comparable to the recorded failure in the NERC reports, which validates the developed fragility model of the transmission tower-line structural system.
(5) Results from both the element and system level indicate that the coupling effect between the transmission tower-line system is not negligible.

In this research, the structural response of the transmission tower-line is considered to be affected by the dynamics of the transmission tower and the transmission tower-line interaction. In the future, the authors plan to refine the simulator by considering more structural influence factors of the power system, such as the breakage of the insulator, the airborne debris, and the impacts from the foundation. Meanwhile, the impact of the different types of transmission towers and spans will be investigated to simulate the system level performance and obtain more realistic and accurate results. Besides, the multi-hazards influence on the power system will be explored to consider the comprehensive impact of the hurricane, rain, and flood on the substations and other power system equipment.

CRediT authorship contribution statement

Jiayue Xue: Conceptualization, Methodology, Formal analysis, Validation, Writing - original draft. **Farshad Mohammadi:** Data curation, Methodology. **Xin Li:** Data curation, Methodology. **Mostafa Sahraei-Ardakani:** Supervision, Writing - review & editing, Funding acquisition. **Ge Ou:** Supervision, Conceptualization, Writing - review & editing, Funding acquisition. **Zhaoxia Pu:** Supervision, Writing - review & editing.

Acknowledgments

The research work described in this paper was supported by Utah's Technology Catalyst (USTAR), award number 18065UTAG004; and the National Science Foundation under award numbers 1839833 and 2004658.

References

[1] National Oceanic and Atmospheric Administration, National Weather Service.

National hurricane center tropical cyclone report hurricane Michael. 2019.
[2] U.S Department of Energy, Infrastructure Security & Energy Restoration. Tropical cyclone Michael report 17. 2018.
[3] Abedi A, Gaudard L, Romerio F. Review of major approaches to analyze vulnerability in power system. Reliab Eng Syst Saf 2019;183:153–72.
[4] Kang C, Xia Q, Xiang N. Sequence operation theory and its application in power system reliability evaluation. Reliab Eng Syst Saf 2002;78(2):101–9.
[5] Volkanovski A, Čepin M, Mavko B. Application of the fault tree analysis for assessment of power system reliability. Reliab Eng Syst Saf 2009;94(6):1116–27.
[6] Salman AM, Li Y, Bastidas-Arteaga E. Maintenance optimization for power distribution systems subjected to hurricane hazard, timber decay and climate change. Reliab Eng Syst Saf 2017;168:136–49.
[7] Salman AM, Li Y, Stewart MG. Evaluating system reliability and targeted hardening strategies of power distribution systems subjected to hurricanes. Reliab Eng Syst Saf 2015;144:319–33.
[8] Ryan PC, Stewart MG, Spencer N, Li Y. Reliability assessment of power pole infrastructure incorporating deterioration and network maintenance. Reliab Eng Syst Saf 2014;132:261–73.
[9] Sperstad IB, Kjølle GH, Gjerde O. A comprehensive framework for vulnerability analysis of extraordinary events in power systems. Reliab Eng Syst Saf 2020;196:106788.
[10] Zio E, Golea LR. Analyzing the topological, electrical and reliability characteristics of a power transmission system for identifying its critical elements. Reliab Eng Syst Saf 2012;101:67–74.
[11] Abedi A, Gaudard L, Romerio F. Power flow-based approaches to assess vulnerability, reliability, and contingency of the power systems: the benefits and limitations. Reliab Eng Syst Saf 2020:106961.
[12] Liu H., Davidson R.A., Rosowsky D.V., Stedinger J.R. Negative binomial regression of electric power outages in hurricanes. J Infrastruct Syst2005; 258–67.
[13] Han SR, Guikema SD, Quiring SM, Lee KH, Rosowsky D, Davidson RA. Estimating the spatial distribution of power outages during hurricanes in the Gulf coast region. Reliab Eng Syst Saf 2009:199–210.
[14] Nateghi R, Guikema S, Quiring SM. Power outage estimation for tropical cyclones: improved accuracy with simpler models. Risk Anal 2014:1069–78.
[15] Liu H, Davidson RA, Apanasovich TV. Spatial generalized linear mixed models of electric power outages due to hurricanes and ice storms. Reliab Eng Syst Saf 2008:897–912.
[16] Quiring SM, Zhu L, Guikema SD. Importance of soil and elevation characteristics for modeling hurricane-induced power outages. Nat Haz 2011:365–90.
[17] Guikema SD, Quiring SM, Han SR. Prestorm estimation of hurricane damage to electric power distribution systems. Risk Anal: Int J 2010:1744–52.
[18] Liu Y, Singh C. A methodology for evaluation of hurricane impact on composite power system reliability. IEEE Trans Power Syst 2010:145–52.
[19] Wang Y, Chen C, Wang J, Baldick R. Research on resilience of power systems under natural disasters—a review. IEEE Trans Power Syst 2015:1604–13.
[20] El-Sharkawi MA. Electric energy: an introduction. 3rd ed. CRC Press; 2012.
[21] Mensah AF, Dueñas-Osorio L. Efficient resilience assessment framework for electric power systems affected by hurricane events. J Struct Eng 2015:C4015013.
[22] Boggess JM, Becker GW, Mitchell MK. Storm & flood hardening of electrical substations. Proceedings of the 2014 IEEE PES T&D conference and exposition. 2014. p. 1–5.
[23] North American Electric Reliability Corporation. Hurricane Harvey event analysis report. 2018.
[24] North American Electric Reliability Corporation. Hurricane sandy event analysis report. 2014.
[25] Winkler J, Duenas-Osorio L, Stein R, Subramanian D. Performance assessment of topologically diverse power systems subjected to hurricane events. Reliab Eng Syst Saf 2010:323–36.
[26] Ahmed A, Arthur C, Edwards M. Collapse and pull–down analysis of high voltage electricity transmission towers subjected to cyclonic wind. Proceedings of the IOP conference series: materials science and engineering. 2010.
[27] Savory E, Parke GA, Zeinoddini M, Toy N. Disney P. Modelling of tornado and microburst-induced wind loading and failure of a lattice transmission tower. Eng Struct 2010:365–75.
[28] Shehata AY, El Damatty AA, Savory E. Finite element modeling of transmission line under downburst wind loading. Finite Elem Anal Des 2005:71–89.
[29] Yang Y, Tang W, Liu Y, Xin Y, Wu Q. Quantitative resilience assessment for power transmission systems under typhoon weather. IEEE Access 2018:40747–56.
[30] Albermani F, Kitipornchai S, Chan RW. Failure analysis of transmission towers. Eng Fail Anal 2009:1922–8.
[31] Fu X, Li HN. Uncertainty analysis of the strength capacity and failure path for a transmission tower under a wind load. J Wind Eng Ind Aerodyn 2018:147–55.
[32] Zhang M, Zhao G, Wang L, Li J. Wind-induced coupling vibration effects of high-voltage transmission tower-line systems. Shock Vib 2017:1–34.
[33] Ellingwood BR, Rosowsky DV, Li Y, Kim JH. Fragility assessment of light-frame wood construction subjected to wind and earthquake hazards. J Struct Eng 2004:1921–30.
[34] Lee KH, Rosowsky DV. Fragility assessment for roof sheathing failure in high wind regions. Eng Struct 2005:857–68.
[35] Lee S, Ham HJ, Kim HJ. Fragility assessment for cladding of industrial buildings subjected to extreme wind. J Asian Archit Build Eng 2013:65–72.
[36] Seo DW, Caracoglia L. Estimating life-cycle monetary losses due to wind hazards: fragility analysis of long-span bridges. Eng Struct 2013:1593–606.
[37] Smith MA, Caracoglia L. A Monte Carlo based method for the dynamic “fragility analysis” of tall buildings under turbulent wind loading. Engineering Structures 2011:410–20.
[38] Fu X, Li HN, Li G. Fragility analysis and estimation of collapse status for transmission tower subjected to wind and rain loads. Struct Saf 2016;58:1–10.
[39] Ma L., Christou V., Bocchini P. Probabilistic simulation of power transmission systems affected by hurricane events based on fragility and AC power flow analyses. 2019;1–8.
[40] Fu X, Li HN, Tian L, Wang J, Cheng H. Fragility analysis of transmission line subjected to wind loading. J Perform Construct Fac 2019:04019044.
[41] Cai Y, Xie Q, Xue S, Hu L, Kareem A. Fragility modelling framework for transmission line towers under winds. Eng Struct 2019:686–97.
[42] Baker JW. Efficient analytical fragility function fitting using dynamic structural analysis. Earthq Spectra 2015:579–99.
[43] Karamlou A, Bocchini P. Computation of bridge seismic fragility by large-scale simulation for probabilistic resilience analysis. Earthq Eng Struct Dyn 2015:1959–78.
[44] Schotanus MIJ, Franchin P, Lupoi A, Pinto P. Seismic fragility analysis of 3D structures. Struct Saf 2004:421–41.
[45] Tort C, Şahin S, Hasançebi O. design of steel lattice transmission line towers using simulated annealing and PLS-TOWER. Comput Struct 2017:75–94.
[46] ASCE. Guidelines for electrical transmission line structural loading. 3rd ed. Virginia, Reston: American Society of Civil Engineering,ASCE:; 2010.
[47] Weather G.Sample transmission tower design. 2019. Accessedhttp://weatherg.utah.edu/.
[48] ANSYS. ANSYS LS-DYNA. 2019. Accessed https://www.ansys.com/products/structures/ansys-ls-dyna.
[49] Zhang Z, Li H, Li G, Wang W, Tian L. The numerical analysis of transmission tower-line system wind-induced collapsed performance. Math Probl Eng 2013:1–11.
[50] Irvine HM. Cable structure. The MIT Press; 1981.
[51] ASCE. Minimum design loads for buildings and other structures. ASCE 7-93; 1994.
[52] Davenport G. The spectrum of horizontal gustiness near the ground in high winds. Q J R Meteorol Soc 1961:194–211.
[53] Holmes JD. Wind loading of structures. CRC Press; 2018.
[54] Mara TG, Hong HP. Effect of wind direction on the response and capacity surface of a transmission tower. Eng Struct 2013:493–501.
[55] Fei Q, Zhou H, Han X, Wang J. Structural health monitoring-oriented stability and dynamic analysis of a long-span transmission tower-line system. Eng Fail Anal 2012:80–7.
[56] Li H, Bai H. Dynamic behavior and stability of transmission tower-line system under wind (rain) forces. China Civ Eng J 2007:31–8.
[57] Durst CS. Wind speeds over short periods of time. Meteorol Mag 1960:181–6.
[58] Sang Y, Xue J, Sahraei-Ardakani M, Ou G. An integrated preventive operation framework for power systems during hurricanes. IEEE Syst J 2019:1–11.
[59] TAMU Electric Grid Test Cases. Available:https://ieeexplore.ieee.org/stamp/stamp.jsp?arnumber=8442880.